MARS GLOBAL DIGITAL DUNE DATABASE: WIND DIRECTION ANALYSIS IN SOUTH POLAR REGION (MC-30)

R. K. Hayward[1], L. K. Fenton[2], and T. N. Titus[1] [1]U.S.G.S. 2255 N. Gemini Dr., Flagstaff, AZ 86001, rhayward@usgs.gov. [2]Carl Sagan Center/Ames Research Center, Moffett Field, CA.

Introduction: Work on the south polar (SP) region (65ºS to 90ºS) of the Mars Global Digital Dune Database (MGD[3]) is nearing completion. As previously reported [1], the SP region will add ~55,000 km^2 of medium to large-size dark dunes and ~15,000 km^2 of smaller dune fields and sand deposits to the previously released equatorial (EQ) and north polar (NP) portions of the database [2, 3, 4]. Here we discuss and compare wind directions, as derived from dune centroid azimuth (DCA), slipface (SF), and wind streak (WS) observations in the SP. We also compare those ground-based wind directions to GCM-modeled wind directions.

Wind Direction Evidence: *Dune Centroid Azimuth.* DCA, a measure of a dune field's relative location within a crater, may indicate the prevailing wind direction during the period of dune field migration across a crater floor, thus preserving a relatively broad, regional record of wind regime [4]. We used ESRI ArcMap® tools to locate the centroid (geographic center) of the crater, the centroid of the dune, and to calculate the azimuth of the line connecting the centroids. Nearly 300 DCAs have been calculated for the 65°S to 90°S region [4]. Dune fields with nearly central locations, dune fields located in topographically complex craters, and dune fields in craters with multiple widely scattered dune fields were not assigned a DCA because they would likely not yield meaningful azimuths.

Slipface Orientation. SF orientation probably indicates the direction of prevailing wind during the latest period of major dune modification, thus preserving a relatively short-term, local record. Assignment of a SF direction does not imply that dunes are currently active. Slipface measurements were made based on either high-resolution images where slipfaces are clearly visible, or the gross morphology of dunes formed by unidirectional winds (i.e. barchan, barchanoid and transverse dunes). We used THEMIS visible-wavelength (VIS, 18 m/pixel resolution), Mars Reconnaissance Orbiter Context Camera (MRO CTX, 6 m/pixel resolution), Mars Orbital Camera Narrow Angle (MOC NA, 1.5 m/pixel resolution), and MRO High Resolution Imaging Science Experiment (HiRISE, 0.5 m/pixel resolution) images to measure ~400 SF directions. For ease of plotting and comparison, we averaged the individual (raw) SFs of similar azimuth (< 45º difference) within each dune field.

Wind Streaks. Wind streaks were first recognized in Mariner imagery [e.g. 5]. Wind streak orientation is influenced by strong near-surface winds and can potentially record seasonal wind direction variations [6]. Thomas and Veverka compared Mariner 9 and Viking images. They described changes in light and dark streaks separated by 3 Martian years, and found varying degrees of change [6]. Greeley et al., [7] compared Viking-derived windstreaks to GCM-modeled winds. Since then, repeat orbital imagery [e.g., 8], as well as Mars Exploration Rover data have been used [e.g., 9] to further study the changes in wind streaks over time. For this study, we measured ~85 WS identified in the Arizona State University THEMIS daytime IR global mosaic (115 m/pixel resolution) [10].

GCM Wind Direction. WS, DCA and SF azimuths are compared to wind directions simulated by the NASA Ames GCM (model description [11]). We used a GCM with low spatial resolution (5° latitude x 6° longitude), so replicating the effects of local topography was not possible. Temporal resolution of the GCM is high, with output 8 times per Martian sol, for one Martian year. We filtered the output to obtain winds with shear stresses > .0225 N/m^2 for comparison with our observed surface trends. Haberle et al. [12] have shown that setting this threshold shear stress in the NASA Ames GCM will lift dust in spatial patterns that qualitatively agree with observed dust storm occurrences. Because relatively few (~2000) modeled winds exceed shear stresses > .0225 N/m^2 in the SP region, here we also consider a second set of GCM data with ~100,000 winds of magnitudes > 10 m/sec.

Discussion: In the following figures, wind directions are represented by arrows pointing in the direction of sediment transport. Wind directions are also discussed in terms of the direction of movement. WS directions display the simplest pattern (Fig. 1). Wind direction flow is predominantly toward the west and north. If we take a broad overview, and look at the GCM as a whole, over 80% of the GCM-modeled winds that exceed the .0225 N/ m^2 threshold flow to the north and <15% flow to the west. When the less stringent 10 m/sec threshold is used, about 55% flow to the north and <15% flow to the west (Fig. 2). Thus the WS-derived flow to the north is consistent with GCM-modeled winds. Flow to the west is not as well supported, even though DCA (like WS) directions show overall patterns of flow to the west, as well as the north. The similarity between GCM and surface observations is interesting because, as mentioned above, the DCA is thought to preserve long term wind trends while a WS is more likely to change seasonally. The majority of SF-derived winds flow to the west, which is compatible with WS and DCA evidence. In contrast, only a small percentage of SF winds flow to the north. This trend remained when SF data were grouped according to whether dune fields occurred inside or outside of craters. This is not surprising since dune fields that occur outside of craters are usually associated with topographic traps that could affect dune-forming winds. These local winds, modified by topography, may have a large influence on SF direction, explaining the lack of consistency between WS, DCA, and GCM.

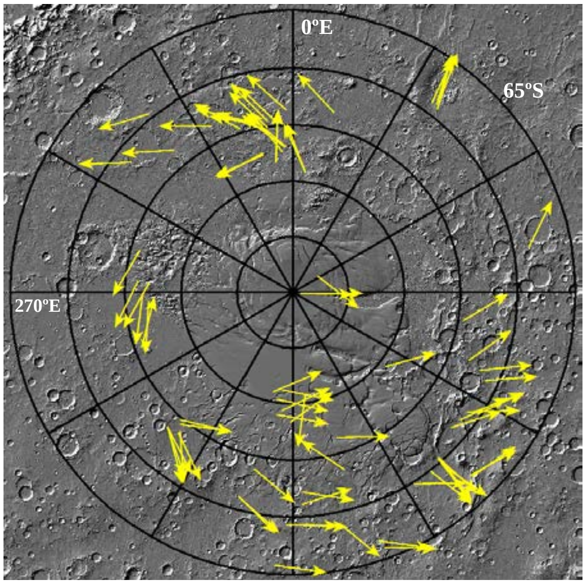

Figure 1. Arrows represent transport direction for WS-derived winds. Majority of winds flow to the west and north. Background is MOLA hillshade. South Stereographic projection.

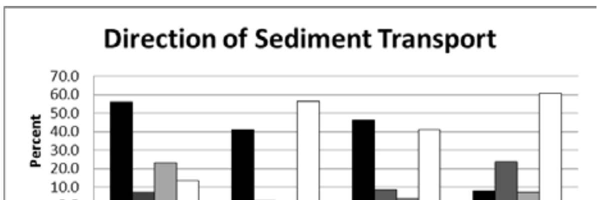

	% GCM>10 m/sec	% WS	% DCA	% Avg SF
N	56.1	41.2	46.4	8.1
E	7.0	2.4	8.7	23.9
S	23.5	0.0	3.8	7.2
W	13.3	56.5	41.2	60.8

Figure 2. Comparison of GCM-modeled winds greater than 10 m/sec and wind direction as measured from windstreak (WS), dune centroid azimuth (DCA), and slipface (SF). Wind directions are given in the direction of sediment transport. N represents winds flowing toward the north with an azimuth of 315º to 45º, E = azimuth of 45º to 135º, S = azimuth of 135º to 225º, W = azimuth of 225º to 315º. GCM, WS and DCA share a strong N component, while WS, DCA and SF share a strong W component.

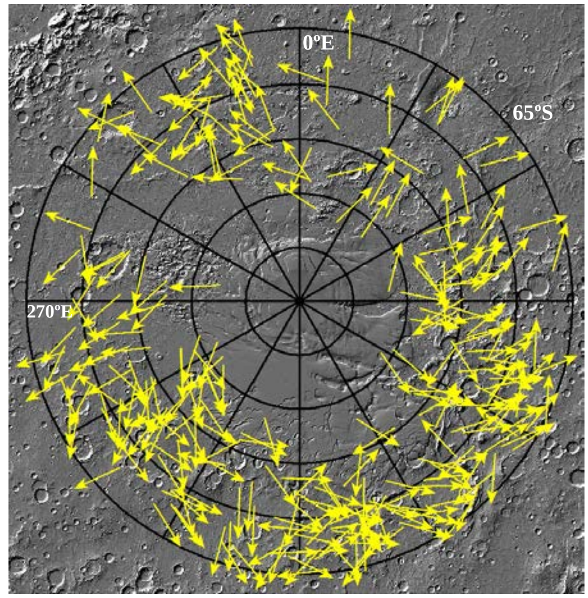

Figure 3. Arrows represent transport direction for DCA-derived winds. Majority of winds flow to the west and north. Background is MOLA hillshade. South Stereographic projection.

Conclusions: 1. The wind directions indicated by the WS and DCA data are most similar. Both show wind directions split almost evenly between winds flowing to the north and to the west. 2. GCM-modeled winds are consistent with the winds flowing north. 3. Like WS and DCA, SF also shows a high percentage of winds flowing to the west (>60%), but unlike WS and DCA, shows only a low percentage of winds flowing north. 4. GCM-modeled winds are not consistent with the SF-derived wind directions suggesting SF-forming winds are strongly influenced by local topography.

References: [1] Hayward et al., 2011, *LPSC XXXXII* Abstract #1051. [2] Hayward R.K., et al. (2007) U.S.G.S. Open File Rep., 2007–1158. [3] Hayward R.K., et al. (2010) U.S.G.S. Open File Rep., 2010–1170. [4] Hayward R.K., et al. (2007) JGR, 112, E11007, doi 10.1029/2007JE002943. [5] Sagan et al., 1972, Icarus, 17, 346-372. [6] Thomas, P. and Veverka, J., 1979, JGR, 84, 8131 - 8146. [7] Greeley et al., 1993, JGR 98, 3183-3196. [8] Toyota, et al., 2011, Planetary & Space Science, doi:10.1016/j.pss.2011.01.015. [9] Geissler et al., 2008, JGR, doi:10.1029/2008JE003102. [10] Christensen, et al., THEMIS Public Data Releases, Planetary Data System node, Arizona State University, http://themis-data.asu.edu. [11] Haberle, R.M., et al. (1999) JGR, 104, 8957-8974. [12] Haberle, R.M., et al. (2003), Icarus 161, 66-89, doi:10.1016/S0019-1035(02)00017-9.